APL MATERIALS 2, 012113 (2014)

Reduction of the thermal conductivity in free-standing silicon nano-membranes investigated by non-invasive Raman thermometry

E. Chávez-Ángel,[1,2] J. S. Reparaz,[1] J. Gomis-Bresco,[1] M. R. Wagner,[1] J. Cuffe,[3] B. Graczykowski,[1] A. Shchepetov,[4] H. Jiang,[5] M. Prunnila,[4] J. Ahopelto,[4] F. Alzina,[1] and C. M. Sotomayor Torres[1,6,a]
[1]*ICN2 – Institut Catala de Nanociencia i Nanotecnologia, Campus UAB, 08193 Bellaterra, Barcelona, Spain*
[2]*Department of Physics, UAB, 08193 Bellaterra, Barcelona, Spain*
[3]*Department of Mechanical Engineering, Massachusetts Institute of Technology, Cambridge, Massachusetts 02139, USA*
[4]*VTT Technical Research Centre of Finland, PO Box 1000, 02044 VTT, Espoo, Finland*
[5]*NanoMaterials Group, Department of Applied Physics and Center for New Materials, Aalto University School of Science, P.O. Box 15100, FI-00076 Aalto, Finland*
[6]*Institució Catalana de Recerca i Estudis Avançats (ICREA), 08010 Barcelona, Spain*

(Received 24 October 2013; accepted 27 December 2013; published online 31 January 2014)

We report on the reduction of the thermal conductivity in ultra-thin suspended Si membranes with high crystalline quality. A series of membranes with thicknesses ranging from 9 nm to 1.5 μm was investigated using Raman thermometry, a novel contactless technique for thermal conductivity determination. A systematic decrease in the thermal conductivity was observed as reducing the thickness, which is explained using the Fuchs-Sondheimer model through the influence of phonon boundary scattering at the surfaces. The thermal conductivity of the thinnest membrane with $d = 9$ nm resulted in (9 $\pm$ 2) W/mK, thus approaching the amorphous limit but still maintaining a high crystalline quality. © *2014 Author(s). All article content, except where otherwise noted, is licensed under a Creative Commons Attribution 3.0 Unported License.* [http://dx.doi.org/10.1063/1.4861796]

The long quest for thermoelectric materials with an improved figure of merit ($ZT = S^2\sigma/\kappa_L + \kappa_e$, where S is the Seebeck coefficient and σ is the electrical conductivity) has mainly followed the roadmap of spoiling the lattice component of the thermal conductivity, κ_L, due to its larger contribution as compared to its electrical counterpart, κ_e, in undoped semiconductors. So far, this concept was based on producing materials with an inherent nanostructuration or simply including defects and/or impurities with the purpose of scattering the acoustic phonons responsible for most of the heat transport, e.g., for Si bulk $\lambda \approx 1$ μm at 300 K.[1,2] This approach was shown to be extremely efficient in a variety of material systems such as, e.g., Bi_2Te_3, PbTe, ZnO, $Si_{1\text{-}x}Ge_x$, and Si.[3,4] Although the case of Si results technologically relevant due to its leading role in the semiconductor industry, its large κ_L in its bulk form of 148 W/mK[5] at room temperature leads to a poor figure of merit of $ZT_{300K} \approx 0.01$. This naturally prevents the use of Si in thermoelectric modules designed for room temperature operation. Many recent publications have demonstrated that by smart engineering of Si in its one- or two-dimensional forms (i.e., nanowires (NWs) or thin films, respectively) it is possible to reduce κ_L by almost two orders of magnitude with respect to its bulk value. The reduction of the thermal conductivity in these systems has been associated to two principal factors: (i) the modification of the acoustic dispersion relations due to the additional periodicity (superlattices and phononic crystal structures)[6–10] or spatial confinement of the phonon

[a]Author to whom correspondence should be addressed. Electronic mail: clivia.sotomayor@icn.cat

 ©Author(s) 2014

© 2015 Author(s). All article content, except where otherwise noted, is licensed under a Creative Commons Attribution (CC BY) license. See: http://creativecommons.org/licenses/by/4.0/ Downloaded to IP: 161.111.180.191 On: Tue, 22 Dec 2015 12:19:57

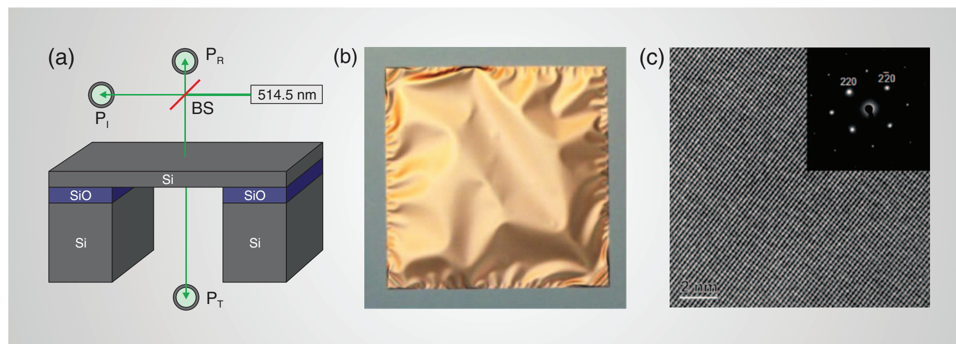

FIG. 1. (a) Schematics of the Si membranes supporting structure and the measurement configuration showing the 514.5 nm incident laser, and the power meters (P_I, P_R, and P_T) used to determine the power absorption coefficient of each membrane. (b) Optical micrographs of a representative Si membrane showing their surface corrugation arising from relaxation of built-in compressive strain. (c) Representative high-resolution transmission electron microscopy (HR-TEM) image of a representative high-stress Si membrane.[11]

modes (thin films and nanowires);[12–14] and (ii) the shortening of the phonon mean free path due to diffuse scattering of phonons at the boundaries.[15–18]

Patterning of suspended Si membranes has shown to be an effective method to decreases the κ_L. Values as low as ∼2 W/mK at room temperature were found in Refs. 10 and 19, thus approaching the amorphous limit of ∼1.8 W/mK.[20] The case of Si nanowires also results exciting due to their large surface-to-volume ratio, i.e., $\kappa_L \approx 7$ W/mK[21] was obtained for NWs with 22 nm in diameter, and $\kappa_L \approx 5$ W/mK was obtained for NWs with 70 nm in diameter and large surface roughness.[22] Although 1D systems such as NWs are ideal regarding κ_L reduction, their applicability to produce devices is by no means straightforward due to the obvious technical complications arising from their manipulation and precise positioning. In fact, Si 2D systems patterned with holes[10,19] led to similar reductions in κ_L as compared to Si NWs.[21–25] However, the necessary patterning stage to introduce efficient phonon scatters (structural holes) introduces a large density of defect centres which might spoil the electrical conductivity of the devices, thus, leading to a poor ZT.

Several previous works have investigated the thermal properties of Si thin films using SOI-based (Silicon-on-Insulator) electrical metrology techniques.[26–29] The in-plane and out-of-plane components of the thermal conductivity were shown to depend on the thickness of the thin films. Although these measurements provided the correct thickness dependence, in most cases several error sources arising from thermal boundary resistances, heat spreading within the heater/thermometers, and heat leakage to the underlying SiO_2 had to be considered and modelled. These problems can be easily overcome using free-standing Si membranes in combination with a contactless method for thermal conductivity determination such as Raman thermometry,[30,31] time-domain thermoreflectance (TDTR),[32,33] frequency-domain thermoreflectance (FDTR),[34] thermal transient grating (TTG),[35] etc. Free-standing ultra-thin Si membranes have recently attracted considerable attention, since they offer model system to study the influence of low dimensionality on the thermal properties as recently reported.[36–38] For example, size effects on the acoustic dispersion relations were investigated by inelastic Brillouin light scattering spectroscopy. A dramatic decrease of at least one order of magnitude of the phase velocity of zero order flexural modes was recently observed,[38] which could have a direct impact on the group velocity and, thus, on the thermal conductivity. Furthermore, reduction of the lifetime of the fundamental dilatational mode (D^1) of about two orders of magnitude was observed by investigating the dynamics of the reflectivity of the membranes using ultrafast methods.[37] Although the flexural and dilatational modes are not the only responsible for the heat transport in the membranes, it is expected that they reflect the influence of size effects in the acoustic branches and, thus, on the thermal properties.

In this work an extra step is taken to account for the influence of low dimensionality in the thermal properties of free-standing ultrathin Si membranes by measuring in a contactless fashion the thermal conductivity, namely, by Raman thermometry. The origin of the size-dependent reduction

© 2015 Author(s). All article content, except where otherwise noted, is licensed under a Creative Commons Attribution (CC BY) license. See: http://creativecommons.org/licenses/by/4.0/ Downloaded to IP: 161.111.180.191 On: Tue, 22 Dec 2015 12:19:57

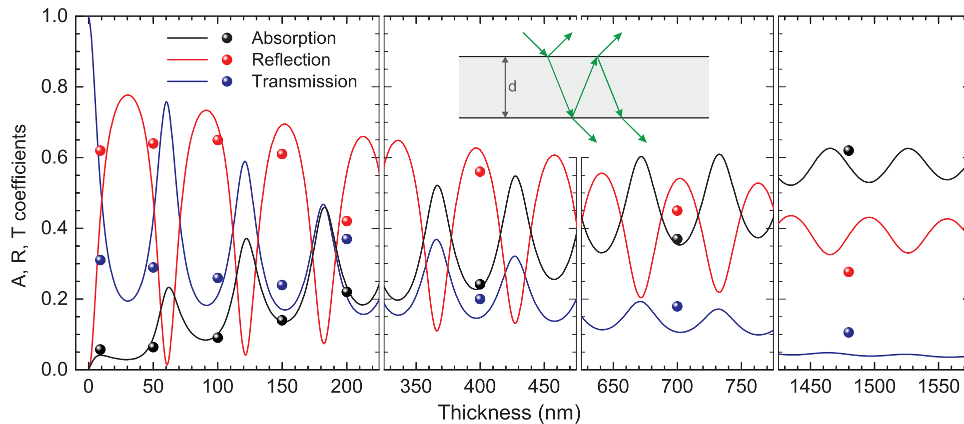

FIG. 2. Power absorption (A), reflection (R), and transmission (T) coefficients as a function of the thickness of the membranes. Solid lines are calculations obtained from the laws of reflection and refraction in a plane-parallel geometry as shown in the inset.

of the thermal conductivity is discussed using the well-established Fuchs-Sondheimer model. This model assumes that the main physical mechanism behind this reduction is the shortening of the phonon mean free path due to diffuse scattering of phonons at the boundaries. For the thinnest membrane with $d = 9$ nm we have observed a 16-fold reduction of the thermal conductivity with respect to the bulk value. Finally, we compare our data with previous experiments in supported Si thin films.

Figure 1(a) shows a schematic of the membranes and the measurements configuration. A SOI substrate was gradually oxidized to thin down the Si film to the desired thickness, followed by removal of the grown oxide. The thermal processes tend to create compressive stress in the Si film, thus leading to buckling of the membranes after release as shown in a representative optical micrograph in Fig. 1(b). We point out that full back etching of the substrate is essential to perform the Raman thermometry measurements, since the absorption coefficient of the membranes must be accurately determined in order to extract the thermal conductivity.

The Raman thermometry technique is based on focusing a laser beam onto the centre of the membranes and monitoring the Raman shift (redshift) of the longitudinal optical (LO) phonon of Si as a function of the absorbed power. The lattice temperature can be directly determined given a previous calibration of these quantities.[39] The thermal conductivity is extracted from the knowledge of the absorbed power and the temperature rise at the spot by solving the 2D heat equation, $\nabla^2 T = P_A/(\kappa \pi a^2 d)e(-(r/a)^2)$ where a is the spot radius and d the thickness of the membranes.[40–45] To obtain the absorbed power in each membrane we first determine their power absorption coefficient. The power absorption (A), reflection (R), and transmission (T) coefficients of the Si membranes as a function of their thickness are shown in Fig. 2. The solid points represent the experimental data. The reflection ($R = P_R/P_I$) and transmission ($T = P_T/P_I$) coefficients were obtained measuring the incident (P_I), reflected (P_R), and transmitted (P_T) powers after focusing the laser spot on the surface of the membranes using a 50× (NA = 0.55) microscope objective. The power absorption (A) coefficient of each membrane was computed considering that $A = 1 - R - T = 1 - P_R/P_I - P_T/P_I$. The absolute error in the determination of A was below 1%. The solid lines in Fig. 2 are the result from theoretical calculations at 300 K obtained applying the laws of reflection and refraction in a plane-parallel film and using the data for the dielectric function of Si reported in Ref. 46. We note that since the thickness of the membranes are well below, or comparable to the wavelength of the incident laser ($\lambda = 514.5$ nm), the membranes behave as Frabry-Pérot optical cavities. For this reason A, R, and T do not exhibit a monotonous response as in the case of bulk Si[39] but rather an oscillatory behaviour. The agreement between the experimental data and the calculated curves results exceptionally good for the power absorption coefficient. We note that the data shown in Fig. 2 were obtained for low excitation powers to ensure no local heating of the membranes. Moreover, the

© 2015 Author(s). All article content, except where otherwise noted, is licensed under a Creative Commons Attribution (CC BY) license. See: http://creativecommons.org/licenses/by/4.0/ Downloaded to IP: 161.111.180.191 On: Tue, 22 Dec 2015 12:19:57

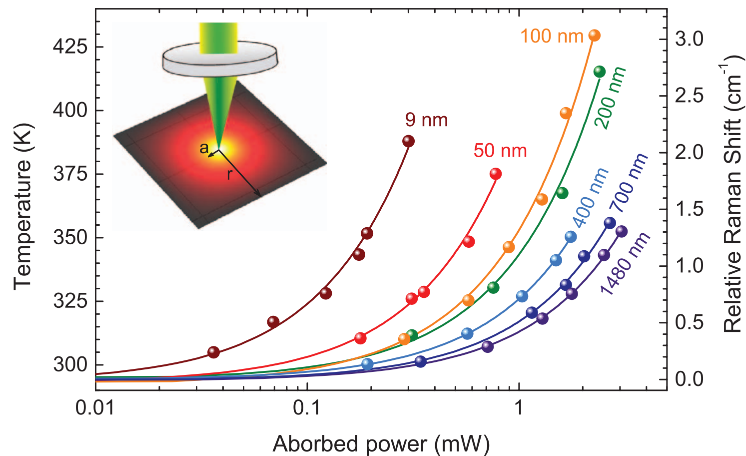

FIG. 3. Raman shift (right axis) of the longitudinal optical (LO) Si phonon of the membranes as a function of the absorbed power and membrane's thickness. The right axis represents the temperature obtained from the temperature dependence of the LO mode extracted from Ref. 35. The full circular symbols represent the low-stress membranes, whereas stars symbols account for the stressed membranes. The inset shows a schematic of the experiments. The incident laser ($\lambda = 514.5$ nm) is focus at the centre of the membranes.

absorption coefficient was also determined as a function of the incident power, since it systematically increases with the local temperature at the laser spot.

Figure 3 displays the temperature of each membrane at the laser spot as a function of the absorbed power, which is computed as $P_A = P_I.A$. The Si LO phonon Raman shift was measured with an accuracy of ± 0.05 cm^{-1} after fitting the spectra with a Lorentzian lineshape. Using the temperature dependence of the Si LO phonon the Raman shift can be converted into local temperature with a corresponding accuracy of about ± 2 K.[39] The solid lines are fits to the data points using a linear relation. For any given absorbed power the temperature rise at the laser spot increases as the thickness of the membranes decreases. The 2D heat equation is solved using finite element (FE) simulations for a given power. We varied the thermal conductivity of each membrane until the temperature rise corresponding to a given power was obtained using the data from Fig. 3. We have chosen a wide range of absorbed powers for each membrane, since in this way the method provides the larger accuracy. Finally, we also show in Fig. 3 a representative solution of the 2D heat equation. The temperature distribution on the membranes exhibits a maximum at the laser spot position and gradually decays to room temperature towards the frame of the membranes, which is in contact with the substrate.

Figure 4 shows the normalized thermal conductivity ($\kappa/\kappa_{\text{Bulk}}$) for the Si membranes as a function of their thickness (d). A systematic decrease is observed with decreasing the thickness, d. The dashed line shows the theoretical prediction of the dependence of κ on d using the Fuchs-Sondheimer model. The details of the calculations are presented in Ref. 47. The agreement between the theoretical model and the experimental data is satisfactory for the lower thicknesses. For the thicker membranes an underestimation is observed, which arises from an artifact of the model, since in this regime boundary scattering becomes gradually negligible. Regarding the influence of surface roughness we surmise that this may also contribute to the reduction of the thermal conductivity. Nevertheless, we expect this effect to be small at room temperature given the <0.5 nm RMS values obtained for all the membranes. A 16-fold reduction of the thermal conductivity ($\kappa_{9\text{nm}} \approx 9$ W/mK) with respect to the bulk value was observed in the thinnest membrane with $d = 9$ nm. In Fig. 4 the experimental data on SOI thin films from Refs. 26–29 as well as in thick Si membranes[30] are also shown for comparison. The thermal conductivities of the SOI thin films are systematically larger than those of the free-standing membranes. This deviation may be associated with the detailed structure of the Si/SiO_2 interface or with a different impurity concentration, but these are not yet experimentally confirmed. A more logical explanation is to consider that in the case of the SOI samples, the substrate acts as an extra heat sink, thus, leading to a larger effective thermal conductivity.

In conclusion, we have investigated the thickness dependence of the thermal conductivity in ultrathin free-standing Si membranes of high crystalline quality using Raman thermometry. The

© 2015 Author(s). All article content, except where otherwise noted, is licensed under a Creative Commons Attribution (CC BY) license. See: http://creativecommons.org/licenses/by/4.0/ Downloaded to IP: 161.111.180.191 On: Tue, 22 Dec 2015 12:19:57

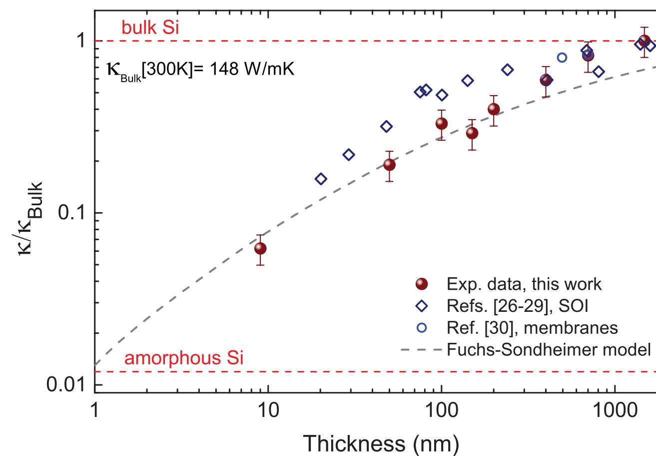

FIG. 4. Thermal conductivities of the membranes, $\kappa/\kappa_{\text{Bulk}}$, normalized to the bulk Si value as a function of the thickness are shown in solid red symbols. The theoretical description of the data using the Fuchs-Sonheimer model is shown in dashed lines. Comparison with previous works on SOI and membranes is also shown. The thermal conductivity of bulk Si was taken as $\kappa_{\text{Bulk}} = 148$ W/mK.[5] The amorphous Si (a-Si) limit is also shown in dotted-dashed line.

power absorption coefficient of the membranes was determined experimentally and theoretically calculated. We have found that the thermal conductivity of the membranes systematically reduces as their thickness decreases. This was successfully modelled considering the shortening of the phonon mean free path due to the diffuse scattering at the boundaries. The thermal conductivity of the thinnest membrane with $d = 9$ nm resulted in (9 ± 2) W/mK, which approaches the amorphous limit while still maintaining a high crystalline quality. The dependence of the thermal conductivity on dimensionality opens new possibilities for building thermoelectric modules based on suspended two-dimensional systems.

The authors acknowledge the financial support from the FP7 project MERGING (Grant No. 309150), the Spanish MICINN projects nanoTHERM (Grant No. CSD2010–0044), TAPHOR (MAT2012–31392), and the Academy of Finland (Grant No. 252598). E.C.-A. gratefully acknowledges a Becas Chile 2010 CONICYT fellowship from Chilean government.

[1] K. Esfarjani, G. Chen, and H. T. Stokes, Phys. Rev. B **84**, 085204 (2011).
[2] K. T. Regner, D. P. Sellan, Z. Su, C. H. Amon, A. J. H. McGaughey, and J. A. Malen, Nat. Commun. **4**, 1640 (2013).
[3] Y. Lan, A. J. Minnich, G. Chen, and Z. Ren, Adv. Funct. Mater. **20**, 357–376 (2010).
[4] A. J. Minnich, M. S. Dresselhaus, Z. F. Ren, and G. Chen, Energy Environ. Sci. **2**, 466 (2009).
[5] C. J. Glassbrenner and G. A. Slack, Phys. Rev. **134**, A1058–A1069 (1964).
[6] M. Maldovan, Phys. Rev. Lett. **110**, 025902 (2013).
[7] E. Dechaumphai and R. Chen, J. Appl. Phys. **111**, 073508 (2012).
[8] C. M. Reinke, M. F. Su, B. L. Davis, B. Kim, M. I. Hussein, Z. C. Leseman, R. H. Olsson III, and I. El-Kady, AIP Adv. **1**, 041403 (2011).
[9] P. E. Hopkins, L. M. Phinney, P. T. Rakich, R. H. Olsson, and I. El-Kady, Appl. Phys. A **103**, 575–579 (2010).
[10] J.-K. Yu, S. Mitrovic, D. Tham, J. Varghese, and J. R. Heath, Nat. Nanotechnol. **5**, 718–721 (2010).
[11] A. Shchepetov, M. Prunnila, F. Alzina, L. Schneider, J. Cuffe, H. Jiang, E. I. Kauppinen, C. M. S. Torres, and J. Ahopelto, Appl. Phys. Lett. **102**, 192108 (2013).
[12] A. Balandin and K. Wang, Phys. Rev. B **58**, 1544–1549 (1998).
[13] M.-J. Huang, T.-M. Chang, W.-Y. Chong, C.-K. Liu, and C.-K. Yu, Int. J. Heat Mass Transfer **50**, 67–74 (2007).
[14] X. Lü, J. Appl. Phys. **104**, 054314 (2008).
[15] G. H. Tang, Y. Zhao, G. X. Zhai, and C. Bi, J. Appl. Phys. **110**, 046102 (2011).
[16] W. Liu and M. Asheghi, Appl. Phys. Lett. **84**, 3819 (2004).
[17] P. Martin, Z. Aksamija, E. Pop, and U. Ravaioli, Phys. Rev. Lett. **102**, 125503 (2009).
[18] P. Hyldgaard and G. D. Mahan, in *Thermal Conductivity*, edited by K. E. Wilkes, R. B. Dinwiddie, and R. S. Graves (Technomics, 1996), Vol. 23, pp. 172–182.
[19] J. Tang, H.-T. Wang, D. H. Lee, M. Fardy, Z. Huo, T. P. Russell, and P. Yang, Nano Lett. **10**, 4279–4283 (2010).
[20] H. Wada and T. Kamijoh, Jpn. J. Appl. Phys. **35**, L648–L650 (1996).
[21] D. Li, Y. Wu, P. Kim, L. Shi, P. Yang, and A. Majumdar, Appl. Phys. Lett. **83**, 2934 (2003).
[22] J. Lim, K. Hippalgaonkar, S. C. Andrews, A. Majumdar, and P. Yang, Nano Lett. **12**, 2475–2482 (2012).
[23] D. L. Nika, E. P. Pokatilov, A. A. Balandin, V. M. Fomin, A. Rastelli, and O. G. Schmidt, Phys. Rev. B **84**, 165415 (2011).

© 2015 Author(s). All article content, except where otherwise noted, is licensed under a Creative Commons Attribution (CC BY) license. See: http://creativecommons.org/licenses/by/4.0/ Downloaded to IP: 161.111.180.191 On: Tue, 22 Dec 2015 12:19:57

[24] D. L. Nika, A. I. Cocemasov, C. I. Isacova, A. A. Balandin, V. M. Fomin, and O. G. Schmidt, Phys. Rev. B **85**, 205439 (2012).
[25] D. L. Nika, A. I. Cocemasov, D. V. Crismari, and A. A. Balandin, Appl. Phys. Lett. **102**, 213109 (2013).
[26] M. Asheghi, Y. K. Leung, S. S. Wong, and K. E. Goodson, Appl. Phys. Lett. **71**, 1798 (1997).
[27] M. Asheghi, M. N. Touzelbaev, K. E. Goodson, Y. K. Leung, and S. S. Wong, J. Heat Transfer **120**, 30 (1998).
[28] Y. S. Ju and K. E. Goodson, Appl. Phys. Lett. **74**, 3005 (1999).
[29] W. Liu and M. Asheghi, J. Appl. Phys. **98**, 123523 (2005).
[30] X. Liu, X. Wu, and T. Ren, Appl. Phys. Lett. **98**, 174104 (2011).
[31] A. A. Balandin, Nature Mater. **10**, 569–581 (2011).
[32] M. G. Burzo, P. L. Komarov, and P. E. Raad, in *Proceedings of the ITherm 2002. Eighth Intersociety Conference on Thermal and Thermomechanical Phenomena in Electronic Systems Cat. No.02CH37258* (IEEE, 2002), pp. 142–149.
[33] M. G. Burzo, P. L. Komarov, and P. E. Raad, Microelectron. J. **33**, 697–703 (2002).
[34] A. J. Schmidt, R. Cheaito, and M. Chiesa, Rev. Sci. Instrum. **80**, 094901 (2009).
[35] J. E. Graebner, Rev. Sci. Instrum. **66**, 3903 (1995).
[36] J. A. Johnson, A. A. Maznev, J. Cuffe, J. K. Eliason, A. J. Minnich, T. Kehoe, C. M. S. Torres, G. Chen, and K. A. Nelson, Phys. Rev. Lett. **110**, 025901 (2013).
[37] J. Cuffe, O. Ristow, E. Chávez, A. Shchepetov, P.-O. Chapuis, F. Alzina, M. Hettich, M. Prunnila, J. Ahopelto, T. Dekorsy, and C. M. S. Torres, Phys. Rev. Lett. **110**, 095503 (2013).
[38] J. Cuffe, E. Chávez, A. Shchepetov, P.-O. Chapuis, E. H. El Boudouti, F. Alzina, T. Kehoe, J. Gomis-Bresco, D. Dudek, Y. Pennec, B. Djafari-Rouhani, M. Prunnila, J. Ahopelto, and C. M. S. Torres, Nano Lett. **12**, 3569–3573 (2012).
[39] *Group IV Elements, IV-IV and III-V Compounds. Part a – Lattice Properties*, edited by O. Madelung, U. Rössler, and M. Schulz (Springer-Verlag, Berlin/Heidelberg, 2001), Vol. A.
[40] S. Chen, Q. Li, Q. Zhang, Y. Qu, H. Ji, R. S. Ruoff, and W. Cai, Nanotechnology **23**, 365701 (2012).
[41] J.-U. Lee, D. Yoon, H. Kim, S. W. Lee, and H. Cheong, Phys. Rev. B **83**, 081419 (2011).
[42] S. Chen, A. L. Moore, W. Cai, J. W. Suk, J. An, C. Mishra, C. Amos, C. W. Magnuson, J. Kang, L. Shi, and R. S. Ruoff, ACS Nano **5**, 321–328 (2011).
[43] P. Dario, in *Proceedings of the 2007 IEEE International Conference on Robotics and Biomimetics (ROBIO)* (IEEE, 2007), pp. 859–863.
[44] S. Chen, Q. Wu, C. Mishra, J. Kang, H. Zhang, K. Cho, W. Cai, A. A. Balandin, and R. S. Ruoff, Nature Mater. **11**, 203–207 (2012).
[45] A. A. Balandin, S. Ghosh, W. Bao, I. Calizo, D. Teweldebrhan, F. Miao, and C. N. Lau, Nano Lett. **8**, 902–907 (2008).
[46] J. Šik, J. Hora, and J. Humlíček, J. Appl. Phys. **84**, 6291 (1998).
[47] See supplementary material at http://dx.doi.org/10.1063/1.4861796 for a detailed description of the calculations. The thickness dependence of the thermal conductivity is described through the Fuchs-Sondheimer model.

© 2015 Author(s). All article content, except where otherwise noted, is licensed under a Creative Commons Attribution (CC BY) license. See: http://creativecommons.org/licenses/by/4.0/ Downloaded to IP: 161.111.180.191 On: Tue, 22 Dec 2015 12:19:57